Chinese Chemical Letters 32 (2021) 3890–3894

Contents lists available at ScienceDirect

Chinese Chemical Letters

journal homepage: www.elsevier.com/locate/cclet

Communication

Rational design of far red to near-infrared rhodamine analogues with huge Stokes shifts for single-laser excitation multicolor imaging

Xingxing Zhang, Tianbing Ren*, Feiyu Yang, Lin Yuan*

State Key Laboratory of Chemo/Biosensing and Chemometrics, College of Chemistry and Chemical Engineering, Hunan University, Changsha 410082, China

ARTICLE INFO

Article history:
Received 21 March 2021
Revised 1 June 2021
Accepted 14 June 2021
Available online 23 June 2021

Keywords:
Fluorescent dyes
Rhodamine analogues
Huge stokes shifts
Single-laser excitation
Multicolor imaging

ABSTRACT

Rhodamine dyes have been widely employed in biological imaging and sensing. However, it is always a challenge to design rhodamine derivatives with huge Stokes shift to address the draconian requirements of single-excitation multicolor imaging. In this work, we described a generally strategy to enhance the Stokes shift of rhodamine dyes by completely breaking their electronic symmetry. As a result, the Stokes shift of novel rhodamine dye DQF-RB-Cl is up to 205 nm in PBS, which is the largest in all the reported rhodamine derivatives. In addition, we successfully realized the single excitation trichromatic imaging of mitochondria, lysosomes and cell membranes by combining DQF-RB-Cl with commercial lysosomal targeting probe Lyso-Tracker Green and membrane targeting dye Dil. This is the organic synthetic dyes for SLE-trichromatic imaging in cells for the first time. These results demonstrate the potential of our design as a useful strategy to develop huge Stokes shift fluorophore for bioimaging.

Fluorescence imaging has been widely used for interrogating living systems owing to its superior sensitivity, fine spatiotemporal resolution, non-invasiveness and low cost [1–6]. In particular, multicolor fluorescence imaging has become a key method to observe the interaction between intramolecular structures and biomolecules and to track different organelles in the same cell [7–9]. Generally, the more colors of multicolor imaging, the more information can be obtained with less experimental throughput [10,11]. However, due to lack of suitable fluorophores with matched excitation wavelength and huge Stokes shifts (> 180 nm), most of the multicolor imaging experiments are multi-laser excitation, and only a few can achieve multi-color imaging with single-laser excitation (SLE) [12–14]. Compared with multi-excitation, single-laser excitation multicolor imaging greatly saves resources and reduces damage to biological samples, especially when there are three or more colors. Up to date, almost all of the multicolor images (more than two colors imaging) with single-laser excitation are based on the Qdots [15] and fluorescent proteins [16]. However, because of the unadjustable targeting and poor stability, their bioimaging applications are seriously restricted. Thus, it is significant and necessary to develop other fluorophores with excellent photophysical properties for SLE-multicolor imaging.

Compared to other typies of fluorophores, organic synthetic dyes, owing to their easy modification and excellent biocompatibility, have received considerable attention for biomolecule detection [17–21] and labeling [7,22,23]. Among them, rhodamine and its derivatives are highly popular because of their outstanding photophysical properties, including high extinction coefficients, good quantum yields, excellent water solubility and resistance to photobleaching [24,25]. However, the traditional rhodamine dyes usually suffered from short emission wavelength (< 600 nm) togerther with small Stokes shifts (< 30 nm), thus makes them difficult for SLE-multicolor imaging. Although rencently many novel rhodamine derivatives with large Stokes shifts (> 60 nm) have been developed and some of them have been used for two-color imaging [14,26–29], there is no reported work with more than two colors imaging. In addition, the excitation wavelengthes do not well match the laser of existing microscope also weakens the value of these new rhodamines. Therefore, it remains an urgent need to design novel rhodamine dyes with excellent photophysical properties for SLE-multicolor imaging.

In this study, by completely breaking the symmetry of traditional rhodamine, we described a strategy to develop rhodamines analogues (DQF-RB-OMe, DQF-RB-H and DQF-RB-Cl) with huge Stokes shift (> 150 nm) and far red to near-infrared emission (FR-NIR, > 650 nm). Especially, DQF-RB-Cl, which was equipped with 1,4-dimethyl-decahydro-quinoxaline (DQ) group and chlorine to the xanthene skeleton, displayed the largest Stokes shift (205 nm in PBS) among all the reported FR-NIR dyes based on rhodamine

* Corresponding authors.
E-mail addresses: rentianbing@hnu.edu.cn (T. Ren), lyuan@hnu.edu.cn (L. Yuan).

https://doi.org/10.1016/j.cclet.2021.06.038
1001-8417/

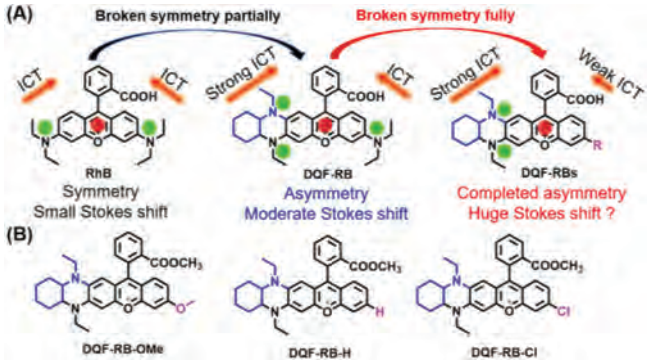

Fig. 1. (A) Rational engineering principle of novel rhodamine dyes. (B) Chemical structures of rhodamine derivatives.

Table 1
Calculated absorption wavelengths, emission wavelengths and oscillator strengths of rhodamine B, DQF-RB, DQF-RB-OMe, DQF-RB-H and DQF-RB-Cl.

Compd.	Absorption (nm)	Oscillator strength	Emission (nm)
Rhodamine B	478 ($S_0 \rightarrow S_1$)	0.9712	504
	403 ($S_0 \rightarrow S_2$)	0.0101	
DQF-RB	545 ($S_0 \rightarrow S_1$)	0.664	675
	436 ($S_0 \rightarrow S_2$)	0.3949	
DQF-RB-OMe	539 ($S_0 \rightarrow S_1$)	0.3175	703
	428 ($S_0 \rightarrow S_2$)	0.5972	
DQF-RB-H	537 ($S_0 \rightarrow S_1$)	0.2558	711
	428 ($S_0 \rightarrow S_2$)	0.5625	
DQF-RB-Cl	547 ($S_0 \rightarrow S_1$)	0.2925	720
	431 ($S_0 \rightarrow S_2$)	0.647	

Note: Absorption wavelength, oscillator strength and emission wavelength were obtained from Gaussian 09 programs at the B3LYP/6–31+G(d) level using a CPCM solvation model with water as the solvent.

Table 2
Photo-physical properties of DQF-RB-OMe, DQF-RB-H and DQF-RB-Cl in EtOH.

Comp.	λ_{abs} (nm)	λ_{em} (nm)	Stokes shift (nm)	ε (L mol^{-1} cm^{-1})	ϕ_f
DQF-RB-OMe	543	680	137	76,000	11%
DQF-RB-H	487	680	193	66,000	3.5%
DQF-RB-Cl	491	685	194	67,000	1.4%

frameworks (Table S1 in Supporting information). DFT calculations indicate that the traditional rhodamines usually are excited to the first excited state and then emit photons. In contrast, DQF-RB-Cl first transits to the second excited state (SES) by absorbing high-energy photons, then jumps from SES to first excited state (FES) through internal conversion (IC) and then, emits photons through the first excited state. This feature makes DQF-RB-Cl have significant blue shifted absorption (485 nm) and red shifted emission (690 nm). As a result, its Stokes shift is deeply expanded. Benefiting from its large Stokes shift, we successfully realized the SLE-trichromatic imaging of mitochondria, lysosomes and cell membranes by combining DQF-RB-Cl with commercial lysosomal targeting probe Lyso-Tracker Green and membrane targeting dye Dil. We believe that this strategy may not only provide a means to construct dyes with huge Stokes shifts, but also reignite interest in multicolor imaging, especially more than two colors imaging with single-laser excitation.

Our previous work has indicated that when an amino group of traditional rhodamine (*e.g.* RhB) is replaced by 1,4-dimethyldecahydro-quinoxaline (DQ) with stronger electron donor group, the Stokes shift (up to 85 nm in PBS) of rhodamine derivative DQF-RB increases significantly (Fig. 1A and Table S2 in Supporting information) [26]. However, for SLE-multicolor imaging, this moderate Stokes shift is not sufficient. Considering that enhanced intramolecular charge transfer (ICT) can effectively increase the Stokes shift of D-A dye and breaking the electronic symmetry could strengthen the rhodamines' ICT process [30–32], here we intend to replace another one diethylamino group of rhodamine (DQF-RB) with a weaker electron-donating group or electron-withdrawing substituent. We expect that this change will further enhance the electronic asymmetry of rhodamine dyes and continue to enhance its unidirectional ICT, thus increasing the Stokes shift of rhodamine derivatives to a greater extent (Fig. 1A). As proof of concept, we designed and synthesized three new rhodamine B derivatives, named as DQF-RB-OMe, DQF-RB-H and DQF-RB-Cl (Fig. 1B). As described in Scheme S2 (Supporting information), all these new rhodamines were synthesized with a simple one-step procedure. And then they were carefully characterized by NMR and ESI analyses.

With the new dyes in hand, we first investigated their photophysical properties in different solvents. As shown in Fig. 2 and Table S2, compared to the original dye DQF-RB, with decreasing electron-donating ability of the donor group, the maximum absorption wavelength of new rhodamine derivatives gradually decreased from 584 nm (DQF-RB) to 534 nm (DQF-RB-OMe) and then to 483 nm (DQF-RB-H) and 485 nm (DQF-RB-Cl). A closer look at the electronic structures in ground state indicates that: Although both the HOMO and LUMO energy levels of the novel rhodamines reduced with the decrease of electron-donating ability of the substituents, the HOMO energy decreased faster than that of LUMO. As a result, their calculated HOMO-LUMO energy gap of these novel rhodamines gradually increased (from 2.53 eV to 2.67 eV) (Fig. 2I), thus resulting the blueshift of their absorption wavelengths. It should also be noted that unlike DQF-RB, which displayed a sharp absorption peak at 584 nm, all of the new rhodamines (DQF-RB-OMe, DQF-RB-H & DQF-RB-Cl) showed broad absorption with two peaks (peak A & peak B) (Figs. 2A-D). This indicated that there may be two absorbed states of the new rhodamines, that is, the absorption from $S_0 \rightarrow S_1$ transition (peak A) and the absorption from $S_0 \rightarrow S_2$ transition (peak B). However, due to the weaker electron-donating ability of hydrogen and chlorine than methoxyl, DQF-RB-H and DQF-RB-Cl exhibited much stronger $S_0 \rightarrow S_2$ transition than $S_0 \rightarrow S_1$ transition (Table 1), whereas the two transitions for DQF-RB-OMe are comparable. This result indicated that with the electronic symmetry of traditional rhodamine further or completely breaked, the absorption of rhodamine dyes gradually changed from $S_0 \rightarrow S_1$ transition to $S_0 \rightarrow S_2$ transition (Table 1).

Thus, the maximum absorption of these new rhodamines undergoes a great blue shift. On the other hand, owing to the asymmetry ICT in the rhodamine skeleton was further enhanced by the weaker electron-donating substituents, the three new rhodamines (DQF-RB-OMe, DQF-RB-H & DQF-RB-Cl) also exhibited a slight red-shift emission (λ_{em} > 685 nm in PBS) compared to their original dye DQF-RB (λ_{em} = 671 nm in PBS) (Fig. S1 and Table S2 in Supporting information). As a result, the calculated Stokes shifts of them are further expanded (> 150 nm), in particular, the Stokes shift of DQF-RB-Cl is up to 205 nm (Table S2), which is the largest Stokes shift among all the rhodamine frameworks (Table S1). It should be also noting that, when completely breaking the symmetry of traditional rhodamine, the fluorescence quantum yields of new rhodamines gradually decreased with the electron-donating ability of substituent weaked (Table 2 and Table S2). This may be due to that as the absorption of the novel rhodamines changed from $S_0 \rightarrow S_1$ transition (DQF-RB & DQF-RB-OMe) to $S_0 \rightarrow S_2$ transition (DQF-RB-H & DQF-RB-Cl), their vibration relaxation and internal conversion were enhanced. As a result, the photons emitted from the excited state back to the ground state greatly decreased. Furthemore, the solvatochromic behaviors showed that the new rhodamine DQF-RB-Cl and DQF-RB-H displayed much more serious fluorescence quenching than that of DQF-RB-OMe, when the sol-

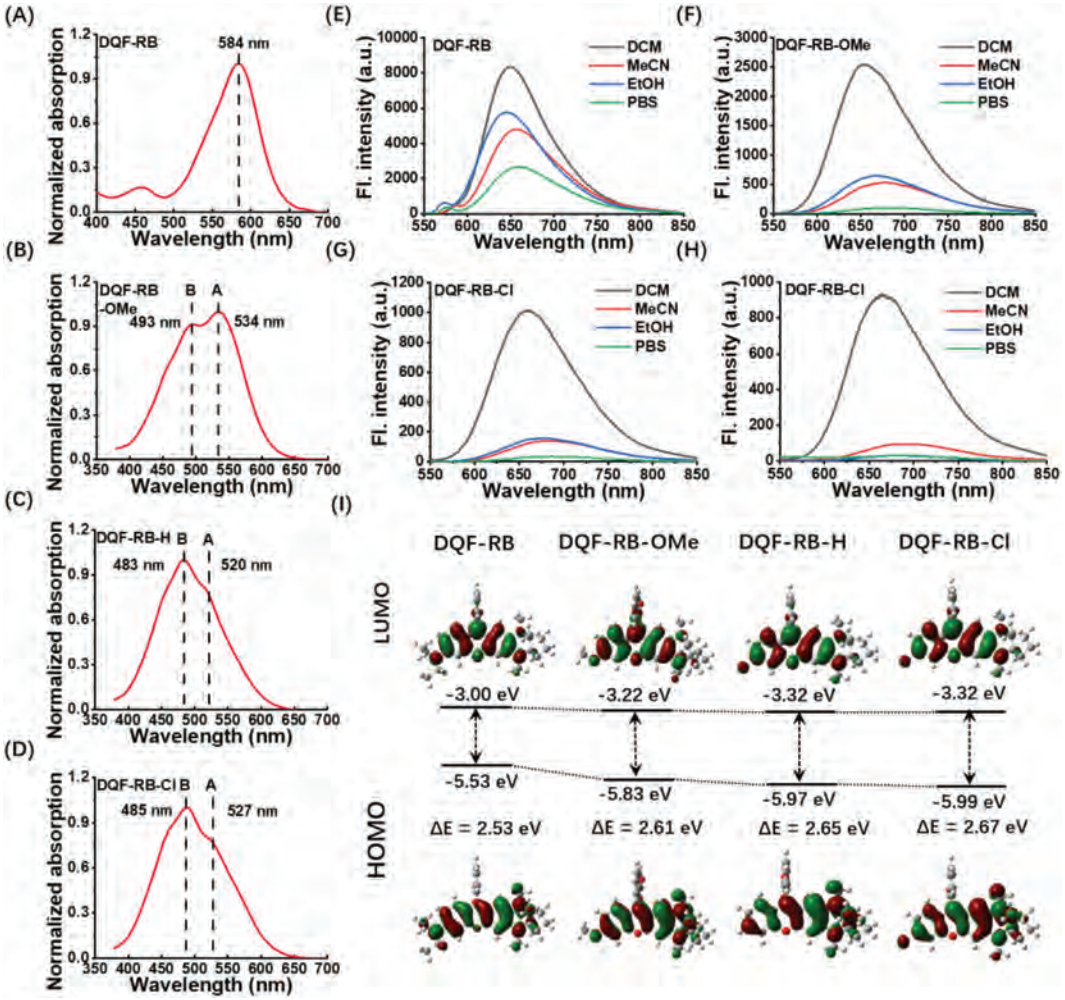

Fig. 2. The normalized absorption spectra of (A) DQF-RB, (B) DQF-RB-OMe, (C) DQF-RB-H, (D) DQF-RB-Cl. Fluorescence emission spectra of (E) DQF-RB, (F) DQF-RB-OMe, (G) DQF-RB-H, (H) DQF-RB-Cl in different solvent. (I) Optimized frontier molecular orbitals and orbital energies of DQF-RB, DQF-RB-OMe, DQF-RB-H and DQF-RB-Cl in the ground state. Water was used as the solvent for calculations at the B3LYP/6–31+G(d) level.

vent polarity is increasing (Figs. 2E-H and Fig. S1g). All these data indicated that further breaking the electronic symmetry of rhodamine derivative DQF-RB by the weaker electron-donating group indeed can increase its asymmetry ICT and prepare new rhodamines with greater Stokes shift (Figs. S3 and S4 in Supporting information). Such discoveries have expanded our understanding of the fluorescent scaffold and allowed us to readily design fluorophores with huge Stokes shift.

Considering that DQF-RB-Cl has the largest Stokes shift (Fig. S3 in Supporting information), we chose it as a representative dye for follow-up experiments. Firstly, we carried out the MTT assay and the result confirmed that even a concentration as high as 10 μmol/L of DQF-RB-Cl would not affect cell viability (Fig. S5 in Supporting information). Next, we tested the photostability of DQF-RB-Cl and the performance was compared with Cy5. DQF-RB-Cl and Cy5 in PBS (25 mmol/L, pH 7.4, containing 1% DMSO) were irradiated continuously by a Xe lamp under the same irradiation conditions. It was observed that DQF-RB-Cl remained highly emissive after continuous irradiation for up to 1 h (99% initial values), whereas the fluorescence intensity of Cy5 decreased to approximately 84% of its initial value under the same power energy (Fig. S6 in Supporting information). To further test the stability of DQF-RB-Cl, we then incubated it with the cells. It can be clearly seen that although the fluorescence of DQF-RB-Cl in the pure PBS was very weak, it still displayed a bright image in living cells. We reason that this significant enhancement may be attributed to the binding between some proteins in the cell with DQF-RB-Cl (Fig. S2 in Supporting information). In addtion, similar to the result in vitro, DQF-RB-Cl incubated within the cells exhibited superior photostability than the contrast dye Cy5 over continuous excitation. Cy5 near completely bleached after 10 min of excitation, whereas DQF-RB-Cl still preserved 70% of initial value (Fig. 3 and Fig. S7 in Supporting information). These results indicated that DQF-RB-Cl possessed more superior photostability than Cy5, and had a

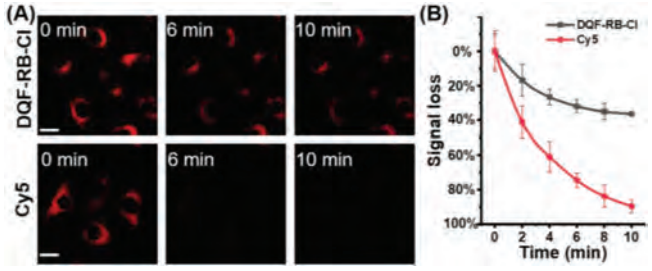

Fig. 3. (A) Confocal fluorescence images of live HeLa cells cultured with DQF-RB-Cl and Cy5 with continuous irradiation using confocal microscope. (B) Quantification of the relative mean fluorescence levels of cells from the images of DQF-RB-Cl and Cy5. Scale bar = 50 μm. For DQF-RB-Cl, λ_{ex} = 488 nm, λ_{em} = 663–738 nm; for Cy5, λ_{ex} = 640 nm, λ_{em} = 663–738 nm. Laser power is 3 mW.

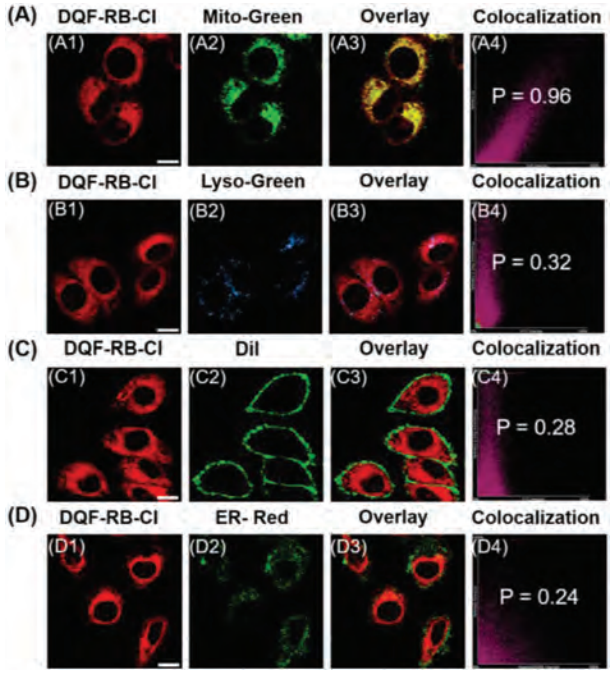

Fig. 4. (A) The colocalization of DQF-RB-Cl in HeLa cells. (A1) Red channel: DQF-RB-Cl (2 μmol/L) stain (λ_{ex} = 488 nm, λ_{em} = 663–738 nm); (A2) green channel: Mito-Tracker Green (200 nmol/L) stain (λ_{ex} = 488 nm, λ_{em} = 500–550 nm); (A3) yellow: overlay; (A4) Pearson's correlation coefficient (r) = 0.96). (B) The colocalization of DQF-RB-Cl in HeLa cells. (B1) Red channel: DQF-RB-Cl (2 μmol/L) stain (λ_{ex} = 488 nm, λ_{em} = 663–738 nm); (B2) blue channel: Lyso-Tracker Green (50 nmol/L) stain (λ_{ex} = 488 nm, λ_{em} = 500–550 nm); (B3) yellow: overlay; (B4) Pearson's correlation coefficient (r) = 0.32). (C) The colocalization of DQF-RB-Cl in HeLa cells. (C1) Red channel: DQF-RB-Cl (2 μmol/L) stain (λ_{ex} = 488 nm, λ_{em} = 663–738 nm); (C2) green channel: Dil (100 nmol/L) stain (λ_{ex} = 560 nm, λ_{em} = 570–620 nm); (C3) yellow: overlay; (C4) Pearson's correlation coefficient (r) = 0.28). (D) The colocalization of DQF-RB-Cl in HeLa cells. (D1) Red channel: DQF-RB-Cl (2 μmol/L) stain (λ_{ex} = 488 nm, λ_{em} = 663–738 nm); (D2) green channel: ER-Tracker Red (100 nmol/L) stain (λ_{ex} = 560 nm, λ_{em} = 570–620 nm); (D3) yellow: overlay; (D4) Pearson's correlation coefficient (r) = 0.24). Scale bar: 20 μm.

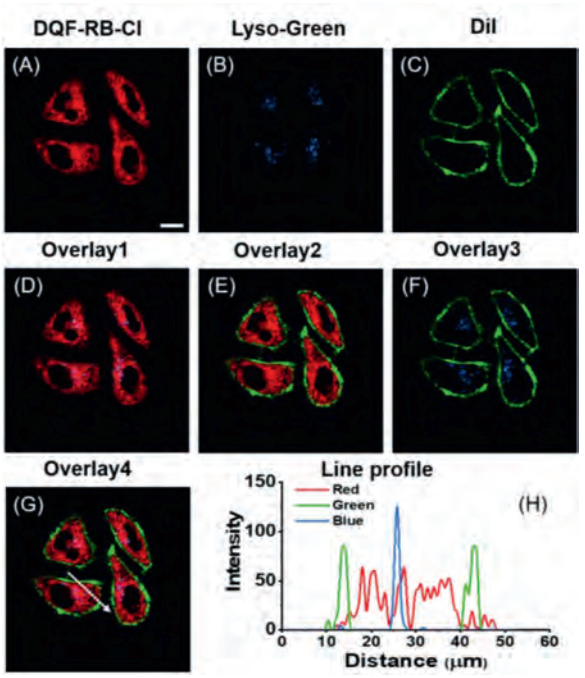

Fig. 5. Confocal SLE-multicolor images in HeLa cells. (A) Red channel: DQF-RB-Cl (λ_{ex} = 488 nm, λ_{em} = 663–738 nm); (B) Lyso-Tracker Green (λ_{ex} = 488 nm, λ_{em} = 500–550 nm); (C) plasma membrane fluorescent probe: Dil (λ_{ex} = 488 nm, λ_{em} = 570–620 nm); (D) the merged image of A, B; (E) the merged image of A, C; (F) the merged image of B, C; (G) the merged image of A, B, C. (H) Line profile: Intensity profile of the white line in image overlap 4. Scale bar: 20 μm.

great potential as an excellent organic fluorophore for the long-term imaging applications.

Given that the positively charged dyes tend to accumulate in the mitochondria [33], we then investigated the viability of DQF-RB-Cl as a mitochondrial targeting reagent. As shown in Fig. 4A and Fig. S8 (Supporting information), after incubation of living HeLa cells with DQF-RB-Cl (2.0 μmol/L) and commercially available Mito-Tracker Green (200 nmol/L) at 37 °C for 15 min, the red fluorescence emitted from DQF-RB-Cl can be well covered with the green fluorescence from Mito-Tracker Green. The high Pearson's coefficient (0.96) of the overlay image indicated that DQF-RB-Cl has a good mitochondrial targeting ability. To further prove its selectivity to mitochondria, DQF-RB-Cl was then incubated with other organelle targeting reagents such as Lyso-Tracker Green, Dil (commercially available membrane targeting dye) and ER-Tracker Red. Figs. 4B-D and Fig. S8 showed that the area marked by DQF-RB-Cl in the cells is significantly distinguished from the lysosomes, membranes and endoplasmic reticulum, and the Pearson's coefficients of their overlapping images are only 0.32, 0.28 and 0.24, respectively. These results indicated that DQF-RB-Cl indeed can localize selectively in mitochondria and could serve as a new kind of mitochondrial trackers. Notably, due to its suitable excitation wavelength (λ_{abs} = 485 nm) and large Stokes shift (205 nm), DQF-RB-Cl and three commercially organelle targeting reagents can be effectively excited by 488-nm laser of the confocal microscope and are collected in different fluorescence channels with no crosstalk (Figs. 4A and B, Fig. S9 in Supporting information). This indicates that DQF-RB-Cl has great potential in the two-color imaging of organelles with single laser excitation.

Encouraged by the above results and huge Stokes shift of DQF-RB-Cl (> 200 nm), we next examined whether it can be used for SLE-trichromatic imaging in cells. Here we choose Lyso-Tracker Green and Dil to image together with DQF-RB-Cl, since they not only have no spectral interference with each other but also exhibit different organelle targeting abilities (Fig. S10 in Supporting information). As shown in Figs. 5A-F, incubation of living HeLa cells with DQF-RB-Cl (2.0 μmol/L), Lyso-Tracker Green (50 nmol/L) and Dil (100 nmol/L) at 37 °C for 15 min, and then collected the red channel (663–738 nm) for DQF-RB-Cl, green channel (570–620 nm) for Dil and blue channel (500–550 nm) for Lyso-Tracker Green. It can be clearly seen that with the 488-nm laser excited, all of the imaging reagents display bright fluorescence in the cells and mark the corresponding organelles very well. From their overlapping images, we can also observe that the fluorescence of the three channels does not seriously overlap, indicating that there is no obvious spectral crosstalk between DQF-RB-Cl and the other two labeling reagents (Figs. 5G and H). These results demonstrated DQF-RB-Cl with huge Stokes shifts can indeed be used for SLE-trichromatic imaging. As far as we know, this is the first case of organic synthetic dye for SLE-trichromatic imaging in cells. From the L02 cells (normal hepatocyte) imaging, we once again confirmed the excellent SLE-trichromatic imaging ability of DQF-RB-Cl (Fig. S11 in Supporting information).

In summary, we report in this study a strategy to develop large Stokes shift rhodamines with far red to near-infrared emission (> 650 nm). With the electronic asymmetry and unidirectional ICT process increases, the novel rhodamine dye DQF-RB-Cl exhibited largest Stokes shift which is up to 205 nm in PBS. Benefiting from its excellent mitochondrial targeting and photostability, DQF-RB-Cl can be applied for the long-term mitochondrial labeling imaging. In addtion, due to its suitable excitation wavelength and

huge Stokes shift, DQF-RB-Cl was successfully applied to the SLE-multicolor imaging (including two-color imaging & trichromatic imaging) in different cells combined with the commercially available Lyso-Tracker Green and membrane targeting dye (Dil) for the first time. We believe that our strategy not only can be used to develop large Stokes shifts rhodamine dyes, but also largely contributes to future improvements of SLE-multicolor imaging .

Declaration of competing interest

We declare that we have no financial and personal relationships with other people or organizations that can inappropriately influence our work, there is no professional or other personal interest of any nature or kind in any product, service and/or company that could be construed as influencing the position presented in, or the review of, the manuscript entitled.

Acknowledgments

This work is supported by the National Natural Science Foundation of China (Nos. 22074036, 22004033, 21877029), the National Postdoctoral Program for Innovative Talents (No. BX20190110) and the China Postdoctoral Science Foundation (No. 2019M662758).

Supplementary materials

Supplementary material associated with this article can be found, in the online version, at doi:10.1016/j.cclet.2021.06.038.

References

[1] T.B. Ren, Z.Y. Wang, Z. Xiang, et al., Angew. Chem. Int. Ed. 60 (2021) 800–805.
[2] X. Luo, J. Li, J. Zhao, et al., Chin. Chem. Lett. 30 (2019) 839–846.
[3] G. Hu, H. Jia, L. Zhao, D.H. Cho, J. Fang, Chin. Chem. Lett. 30 (2019) 1704–1716.
[4] D. Chen, W. Qin, H. Fang, et al., Chin. Chem. Lett. 30 (2019) 1738–1744.
[5] H. Zhou, S. Li, X. Zeng, et al., Chin. Chem. Lett. 31 (2020) 1382–1386.
[6] W. Xu, Z. Zeng, J.H. Jiang, Y.T. Chang, L. Yuan, Angew. Chem. Int. Ed. 55 (2016) 13658–13699.
[7] M. Collot, T.K. Fam, P. Ashokkumar, et al., J. Am. Chem. Soc. 140 (2018) 5401–5411.
[8] X. Chen, X. Zhang, H.Y. Wang, Z. Chen, F.G. Wu, Langmuir 32 (2016) 10126–10135.
[9] W. Chi, J. Chen, W. Liu, et al., J. Am. Chem. Soc. 142 (2020) 6777–6785.
[10] H.Y. Wang, X.W. Hua, H.R. Jia, et al., ACS Biomater. Sci. Eng. 2 (2016) 987–997.
[11] C. Steinmetzger, N. Palanisamy, K.R. Gore, C. Hobartner, Chem. Eur. J. 25 (2019) 1931–1935.
[12] J.B. Grimm, A.N. Tkachuk, L. Xie, et al., Nat. Methods 17 (2020) 815–821.
[13] G. Lukinavicius, L. Reymond, K. Umezawa, et al., J. Am. Chem. Soc. 138 (2016) 9365–9368.
[14] A.N. Butkevich, G. Lukinavicius, E. D'Este, S.W. Hell, J. Am. Chem. Soc. 139 (2017) 12378–12381.
[15] E.R. Goldman, A.R. Clapp, G.P. Anderson, et al., Anal. Chem. 76 (2004) 684–688.
[16] T. Kogure, S. Karasawa, T. Araki, et al., Nat. Biotechnol. 24 (2006) 577–581.
[17] T.B. Ren, S.Y. Wen, L. Wang, et al., Anal. Chem. 92 (2020) 4681–4688.
[18] P. Lu, X. Zhang, T. Ren, L. Yuan, Chin. Chem. Lett. 31 (2020) 2980–2984.
[19] L. Wang, L. Yuan, X. Zeng, et al., Angew. Chem. Int. Ed. 55 (2016) 1773–1776.
[20] W. Chi, Q. Qiao, C. Wang, et al., Angew. Chem. Int. Ed. 59 (2020) 20215–20223.
[21] W. Zhou, X. Fang, Q. Qiao, et al., Chin. Chem. Lett. 32 (2021) 943–946.
[22] P.C. Saha, T. Chatterjee, R. Pattanayak, et al., ACS Omega 4 (2019) 14579–14588.
[23] L. Wang, M. Tran, E. D'Este, et al., Nat. Chem. 12 (2020) 165–172.
[24] M. Li, S. Long, Y. Kang, et al., J. Am. Chem. Soc. 140 (2018) 15820–15826.
[25] L. Wang, W. Du, Z. Hu, et al., Angew. Chem. Int. Ed. 58 (2019) 14026–14043.
[26] T.B. Ren, W. Xu, W. Zhang, et al., J. Am. Chem. Soc. 140 (2018) 7716–7722.
[27] W. Chen, S. Xu, J.J. Day, D. Wang, M. Xian, Angew. Chem. Int. Ed. 56 (2017) 16611–16615.
[28] C. Liu, X. Jiao, Q. Wang, et al., Chem. Commun. 53 (2017) 10727–10730.
[29] Y. Song, H. Zhang, X. Wang, et al., Anal. Chem. 93 (2021) 1786–1791.
[30] A. Gandioso, S. Contreras, I. Melnyk, et al., J. Org. Chem. 82 (2017) 5398–5408.
[31] Y. Yu, J. Wang, H. Xiang, et al., Dyes Pigm. 183 (2020) 108710.
[32] Y. Zhang, S. Xia, M. Fang, et al., Chem. Commun. 54 (2018) 7625–7628.
[33] S.E. Brown, M.F. Ross, A. Sanjuan-Pla, et al., Free Radic. Biol. Med. 42 (2007) 1766–1780.